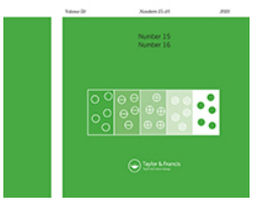
Taylor & Francis
Taylor & Francis Group

SEPARATION SCIENCE AND TECHNOLOGY

Separation Science and Technology



ISSN: 0149-6395 (Print) 1520-5754 (Online) Journal homepage: www.tandfonline.com/journals/lsst20

Facile approach for novel TFC-NF membranes preparation using water soluble poly(vinyl alcohol-*co*-styrenesulfonic acid) and their characterizations

Rikarani R Choudhury, Jaydevsinh M. Gohil & Hiren Raval

To cite this article: Rikarani R Choudhury, Jaydevsinh M. Gohil & Hiren Raval (2023) Facile approach for novel TFC-NF membranes preparation using water soluble poly(vinyl alcohol-*co*-styrenesulfonic acid) and their characterizations, Separation Science and Technology, 58:15-16, 2824-2836, DOI: 10.1080/01496395.2023.2240500

To link to this article: https://doi.org/10.1080/01496395.2023.2240500

Published online: 25 Jul 2023.

Submit your article to this journal

Article views: 139

View related articles

View Crossmark data

Full Terms & Conditions of access and use can be found at
https://www.tandfonline.com/action/journalInformation?journalCode=lsst20

SEPARATION SCIENCE AND TECHNOLOGY
2023, VOL. 58, NOS. 15–16, 2824–2836
https://doi.org/10.1080/01496395.2023.2240500

Taylor & Francis
Taylor & Francis Group

Check for updates

Facile approach for novel TFC-NF membranes preparation using water soluble poly(vinyl alcohol-*co*-styrenesulfonic acid) and their characterizations

Rikarani R Choudhury [a], Jaydevsinh M. Gohil [b,c], and Hiren Raval [d]

[a]CIPET: SARP, Laboratory for Advanced Research in Polymeric Materials (LARPM), Bhubaneswar, Odisha, India; [b]CIPET: SARP, Advanced Polymer Design and Development Research Laboratory (APDDRL), Bengaluru, Karnataka, India; [c]CIPET: SARP, Advanced Research School for Technology and Product Simulation (ARSTPS), Chennnai, Tamil Nadu, India; [d]Membrane Science and Separation Technology Division, CSIR-Central Salt and Marine Chemicals Research Institute (CSIR-CSMCRI), Bhavnagar, Gujarat, India

ABSTRACT

This research article first time reports the concept of thin film composite (TFC) membranes preparation using novel functional copolymer based on poly(vinyl alcohol-*co*-styrenesulfonic acid) (PVA-*co*-SSA). Polysulfone ultrafiltration membrane was coated by applying PVA-*co*-SSA solution via eco-friendly method. The selective coating layer was crosslinked by glutaraldehyde (GA) aqueous solution. The effects of PVA-*co*-SSA and GA solution concentrations used for TFC membranes preparation were evaluated to study the membranes' characteristics. Infrared and Raman spectroscopy was used to confirm the structural characteristics of composite membranes. The resultant TFC membranes were found hydrophilic (exhibited water contact angle in the span of 41° to 60°) and possessed a smooth surface having surface roughness ranging from 20.9 to 26.3 nm with the selective layer thickness in the range of 123 to 276 nm. Membrane exhibited maximum water flux of 32.78 l m^{-2} h^{-1} at when operated in cross-flow cell at 0.69 MPa; at same pressure the membrane gave 74.8% rejection of $MgSO_4$ when fed with 1000 ppm solution of $MgSO_4$; while NaCl rejection of membranes was in the range of 33.75 to 54% when tested using 2000 ppm NaCl feed solution supplied at operating pressure of 1.7 MPa. The trade-off relationship between membrane solute rejection and flux was observed, and composite membranes showed higher rejection of bivalent salt i.e. $MgSO_4$ compared to monovalent salt i.e. NaCl.

ARTICLE HISTORY
Received 15 March 2023
Accepted 19 July 2023

KEYWORDS
eco-friendly technique; thin film composite membrane; polysulfone; PVA-*co*-SSA; nanofiltration; glutaraldehyde

Introduction

Thin film composite (TFC) membrane(s) (TFCMs) prepared through the interfacial polycondensation (IP) reaction concept, are extensively being used to desalinate brackish as well as seawater on commercial scale.[1] A typical polyamide-nanofiltration and reverse osmosis (RO) TFCMs made by IP process consist of layered structure containing (i) a bottom mechanical support made of polyester non-woven fabric of about 100 µm thickness, (ii) a middle microporous ultrafiltration (UF) or microfiltration membrane made of polysulfone (PSF) or polyethersulfone of about 50 µm thickness, and (iii) a top selective layer of PA of about 100–300 nm thickness (deposited by IP).[2] In some cases, an extra thin layer of sulfonated polymer is also applied onto the top selective layer to impart antifouling properties to TFCM. All these layers in TFCM can be independently tailored either by varying (i) type of materials, (ii) thickness of rejection layer, (iii) degree of crosslinking of the top layer, (iv) incorporation of various inorganic and organic additives and nanomaterials in the top and middle layer, (v) surface modification of the top and middle layer, and (vi) incorporation of another coating-layer on the top of the selective-layer and/or at the interface between the top and middle layer.[3–7] Further, in the search of a high-flux and selective membrane, and to improve antifouling properties of the composite membranes, various surface modification approaches, and the use of novel polymeric materials have been investigated.[5] Hydrophilic functional polymers namely poly(vinyl alcohol) (PVA), sulfonated PSF, chitosan, polyethyleneimine, and zwitterion polymers have been studied to fabricate TFCMs for improvement in antifouling and separation characteristics. Among all, the PVA-based TFCMs prepared through grafting, crosslinking, and nanoscale material inclusion techniques found potential applications for NF and RO applications.[5,8] Another interesting material is sulfonated polymers, which have been used to form a selective layer to impart hydrophilicity and charged functional groups onto the NF and RO membranes' surface that subsequently resulted in improving the

CONTACT Jaydevsinh M. Gohil jay21480@yahoo.co.in CIPET: SARP - Advanced Polymer Design and Development Research Laboratory (APDDRL), 7P, Hi-Tech Defence and Aerospace Park, Bengaluru, Karnataka 562149, India

© 2023 Taylor & Francis Group, LLC

selectivity and antifouling properties of membrane.[9–11] There are two types of PVA-based membranes reported in literature, first type is a self-standing thin film membrane without any support.[12–14] This type of membrane usually has nanoporous asymmetric morphologies,[15] and has been studied for NF, RO, and forward osmosis applications for fundamental studies on structure-properties of membrane in absence of any mechanical support. While for more practical application of PVA-based membrane, a second type of membrane is TFC, wherein, a PVA-based coat can be applied as a surface selective layer, an intermediate-layer or both.[8,16] In both categories of theses membranes, to prevent dissolution of PVA layer as well as to maintain its solute rejection characteristics, it is necessary to keep PVA thin film intact during separation application. This is most widely achieved by incorporation of other polymers and/or nanomaterials into the top PVA-based separating layer and by crosslinking this selective-layer.

Preparation of PVA-polyamide TFC membranes has been studied, wherein, PVA is added in aqueous solution containing amines monomer and subsequent IP reaction at the aqueous/organic phase interface produces active layer of cross-linked PVA-polyamide.[17,18] Here, monomer trimesoly chloride present in organic phase usually acts as a crosslinker and a network former of the PVA-PA matrix. Other than PA as active-layer of TFC membranes, an active-layer of TFCM made from the blend of PVA with sodium alginate,[19,20] polyquaternium,[21] and Aquaporin[22] have been reported, all these membranes were cross-linked using glutaraldehyde (GA) at room temperature. Crosslinking of PVA-based various composite and nanocomposite membranes also achieved using boric acid,[23] Zn(II),[23] maleic acid,[24] aconitic acid,[25] 1,6-hexamethylene diisocyanate,[26] and phthalic acid.[25] Membranes preparations using carboxylic acid as a crosslinker necessitate heat treatment to from ester crosslinks.

Similar to PVA-based membranes, sulfonated polymers have been studied to prepare hydrophilic composites membranes.[27,28] Fabrication of TFC NF membranes by IP reaction between trimesoly chloride dissolved in organic phase and piperazine solubilized in aqueous phase containing poly(styrenesulfonic acid) (PSSA),[29,30] and these membranes showed potential for water softening applications. This is due to presence of negatively charged ionic groups such as sulfonic acid ($-SO_3H$) on membrane surface that imparts selectivity between monovalent and bivalent salts. Another class of sulfonated polymers which has been used for TFC membrane preparation are sulfonated pol(arylene ether sulfone),[31] and sulfonated PVA.[32] These types of membranes exhibited a high chlorine tolerance and improved antifouling characteristics than commercial PA-TFC membranes.

Chemical modification of membrane surfaces with PVA-based and sulfonated-polymers results in enhancement in antifouling and chlorine resistance of TFC membranes, however, such type of the additional layer on the TFC membrane aids diffusional mass transfer resistance and decrease the water transport rate. The key objective of this study is to primarily investigate usefulness of PVA-*co*-SSA composite membranes for water treatment. Second prospective is to use water soluble polymer and crosslinker formulation for membrane preparation. Hence, this research article first time describes the studies on the use of novel copolymer, poly (vinyl alcohol-*co*-4-styrenesulfonic acid) (PVA-*co*-SSA) for preparation of TFCM by eco-friendly technique. Similar to the concept of IP technique, here, in this study composite membranes were fabricated by first applying water soluble PVA-*co*-SSA coating onto the PSF UF membrane support, and in the second step, an aqueous GA solution is contacted to induce crosslinking. This concept avoided the use of organic solvent such as hexane for membrane preparation and thereby provided eco-friendly route to fabricate TFCM, and resultants membranes has been characterized to evaluate physiochemical characteristics, salt rejection, and water flux.

Experimental

Materials

PSF-based tight UF support membrane (Molecular weight cutoff, MWCO, of about 20,000 Dalton, Dow Chemicals, USA) was obtained from Prova Technotrade Pvt. Ltd., Mumbai. Copolymer PVA-*co*-SSA (M_w: 270926 and polydispersity index: 2.84) synthesized in our laboratory as reported in elsewhere.[33] GA, 25% aqueous solution (Grade-II), was obtained from Sigma-Aldrich, India. Sodium chloride (NaCl), (80–83% pure) and Magnesium Sulphate ($MgSO_4$), (extra pure) were procured from HI-MEDIA Laboratories, India. Deionized (DI) water was used for preparation of feed solutions as well as polymer and GA solutions.

Preparation of TFCM based on PSF/PVA-co-SSA/GA

PSF UF membrane of MWCO 20,000 Dalton was employed as a substrate membrane for the preparation of TFCM. Support membrane of about 15 cm × 10 cm was cut and its top-surface was contacted with aqueous solution of PVA-*co*-SSA for three mins. Thereafter,

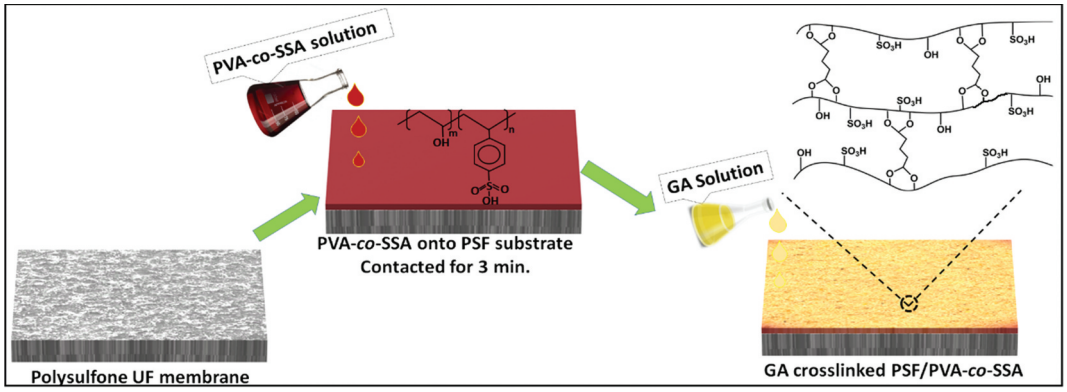


Figure 1. Schematic of PVA-*co*-SSA/GA coating onto the PSF UF substrate for TFC membrane preparation.

Table 1. Concentration of dope solution and crosslinker used for preparation of PSF/PVA-*co*-SSA/GA based composite membranes.

Membrane	PVA-*co*-SSA Solution (wt.%)	GA Solution (wt.%)
1A	2.5	2
1B	1.5	2
1C	1	1
2A	2	6
2B	2	4
2C	2	2

excesses solution of PVA-*co*-SSA from the PSF membrane surface was drained by keeping the membrane in vertical position for about 1 min followed by drying at room temperature for about 20 min. In the second step, to induce crosslinking through acetal formation in the surface of PSF membrane coated with PVA-*co*-SSA, was contacted with aqueous solution of GA (pH ~ 3) for about 45 s, then excess GA solution was drained by keeping membrane in vertical position for 1 min. Resultant membrane heat-treated at 75–80°C for about 5 min by keeping in a hot-air oven, and subsequently, crosslinked membrane was stored at room temperature for 24 h. Finally, membrane was rinsed using DI water and dried at 40°C in a conditioning chamber for about 12 h. The schematic of the developed TFCM is represented in Fig. 1. The different TFCMs were prepared by changing the concentration of PVA-*co*-SSA and GA aqueous solutions, and the membrane formulations and designations are listed in Table 1. A neat PSF UF membrane is abbreviated as a S0.

Characterizations of PSF/PVA-co-SSA/GA based TFCM

The PSF/PVA-co-SSA/GA based TFCMs were initially characterized by Fourier-transform infrared spectrometer (Thermo Nicolet 6700, Smart Orbit, USA) in attenuated total reflection mode in the frequency scan-range of 500–4000 cm^{-1}, at 5 cm^{-1} resolutions. Membrane analysis using Raman spectrometer was performed using Nicolet iS50 (USA) equipped with Nd: YAG diode laser of wavelength 1064 nm. All samples were scanned in the range of 50–4000 cm^{-1} at 8 cm^{-1} resolutions using laser power of 0.05 W. The static contact angle of TFCM' surfaces was studied using Contact Angle Goniometer (APEX Instrument, Dataphysics, Germany), keeping the top surface of membrane up-side, membrane was fixed to the flat glass surface with the help of double-sided tape, droplet of DI water was put on the membrane surface by automatic syringe. Topographical and cross-sectional micrographs of TFCMs were obtained using field-emission gun-scanning electron microscope (GeminiSEM300-ZEISS, Germany). A sample, for membrane cross-section examination was prepared by immersing the membrane-sample in liquid nitrogen for cryogenic fracture. Before FE-SEM analysis, both the types of samples were sputter-coated with gold-palladium for conductive coating (SC7620 Sputter coater) to minimize the charging effect. Atomic Force Microscope (AFM), (XE-100, Park Systems, South Korea) was employed to obtain surface features of the TFCM in non-contact mode (scan area 10 μm × 10 μm). A cantilever with a sharp tip having spring constant, length, a nominal curvature of tip radius, and resonance frequency of 42 N m^{-1}, 125 μm, 10 nm, and 330 kHz respectively was used to scan surface. The membrane samples were dipped in 0.1 mM KCl solution prepared

in deionized water overnight and then zeta potential of the membranes were evaluated using zeta potential analyzer (ZetaCAD) by CAD instruments.

Performance of TFCMs was evaluated in a cross-flow cell (Membrane Test Skid, Tech Inc., Chennai, and CSIR-CSMCRI, Bhavnagar), however, prior to the testing, the TFCMs were dipped into DI water for 12 h, and the flat sheet membrane in wet condition was assembled into the cross-flow cell. Desalination performance i.e., water flux and salts rejection, of the TFCMs was evaluated by supplying feed solution of 2000 ppm NaCl (at 1.7 MPa) and 1000 ppm $MgSO_4$ (at 0.69 and 1.7 MPa) solutions to the test cell. The permeate and feed solution conductivities were measured by conductivity meter (ELICO®, CM 183EC-TDS Analyzer) to calculate the concentrations of solute in both the streams, and flux and rejection characteristics of membrane were calculated as follows using eq. (1) and (2):

$$\text{Flux } \left(lm^{-2}h^{-1}\right) = \frac{V_p}{A_{TFCM} \times t} \tag{1}$$

$$\text{Rejection } (\%) = \frac{C_{feed} - C_{permeate}}{C_{feed}} \times 100 \tag{2}$$

where V_p indicates volume of permeate (in L) collected for over a time period t (in h), and A_{TFCM} represents an active area of membrane (m^2). C_{feed} and $C_{permeate}$ are the feed and permeate solution concentration (gL^{-1}), respectively, calculated from the conductivity data of feed and permeate solutions respectively.

Results and discussions

Concept of PVA-co-SSA crosslinking using GA

Conceptually, the composite PA membrane fabrication by the IP involves the reaction between monomers present in the organic and aqueous phase at the interface. This condition is achieved by contacting the substrate membrane sequentially with the aqueous phase and organic phase monomer solution to form of a nanoporous thin PA film.[4,7] Here, this study includes the use of water-soluble polymers such as PVA-*co*-SSA containing reactive hydroxyl functional group. It is believed that presence of reactive hydroxyl groups in constituting unit (i.e., PVA) of PVA-*co*-SSA has a potential to form network structure (cross-linked) when reacted with aldehyde groups of GA. This phenomenon was established by adding 2–3 drops of GA solution (25%) in a 10 ml PVA-*co*-SSA solution (2% w/v) contained in the test tube, after some time solution in test tube become cloudy and converted into semisolid gel due to crosslinking of PVA-*co*-SSA by GA (Fig. 2). This is due to fact that aldehyde groups (−CHO) of GA condenses with the hydroxyl (−OH) groups present on PVA-*co*-SSA copolymer chain forming acetal linkage. This reaction generally takes place at room temperature in presence of acid catalyst i.e., acidic solution.

Chemical structure of PSF/PVA-co-SSA/GA TFCMs

The chemical structure of PVA-*co*-SSA based selective layer crosslinked by GA and its presence on the PSF support was verified by the FTIR spectroscopy and Raman microscopy analysis. Typical FTIR spectra of support and composite membrane is given in Fig. 3. The various chemical bonds present in PSF membrane (denoted as S0) are identified at 1654 cm^{-1} (attributed to – C=C present in aromatic ring), 1577 cm^{-1} (assigned to – C-C of aromatic ring), 1484 cm^{-1} (-CH_3 group), 1406 cm^{-1} (appeared due to -S=O bond-stretching), 1238 cm^{-1} (-C-O-C- bond-stretching), 1148 cm^{-1} (-S-O-S vibrations), and 1010 and 834 cm^{-1} (aromatic – CH stretching).[34] Similarly, the aromatic carbon stretching, -SO_2 and – SO_3 stretching along with acetal linkage frequencies for PVA-*co*-SSA[33] have been overlapped and merged with corresponding characteristics peaks of PSF, which in turn resulted in more intensities bands than the PSF membrane as observed in Fig. 3(a)

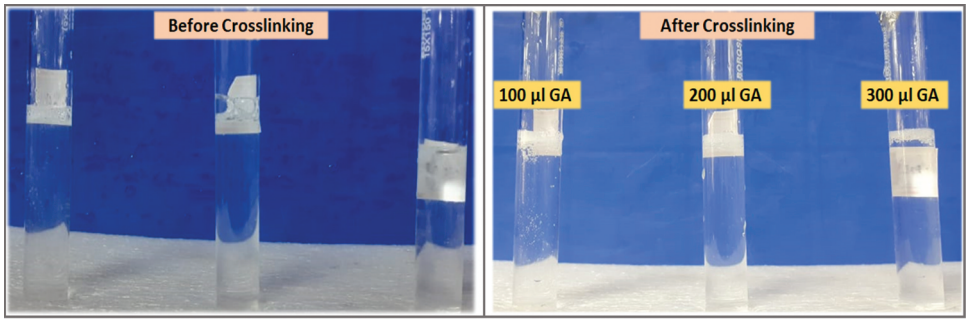


Figure 2. Shows PVA-co-SSA clear solution before addition of GA (left side images), and gelation of PVA-*co*-SSA was observed after adding GA (right side image) due to crosslinking.

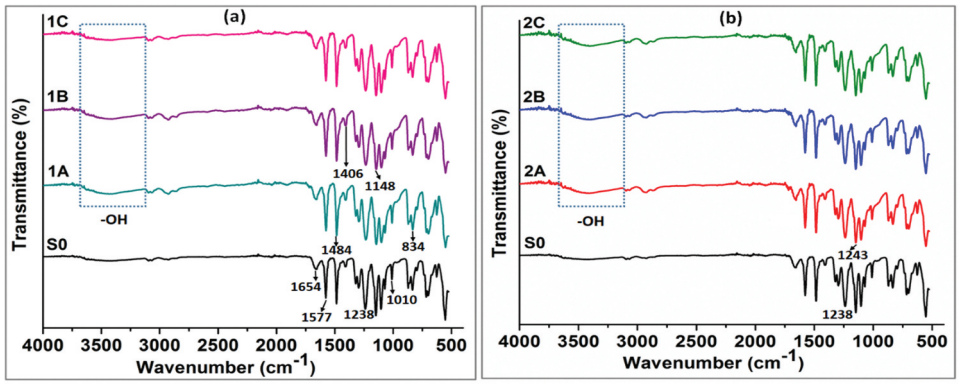


Figure 3. FTIR spectra of bare PSF (S0) and PSF/PVA-*co*-SSA/GA composite membranes (a) 1A, 1B, and 1C, and (b) 2A, 2B, and 2C.

and (b). Appearance of slight shifting of –C-O-C peak from 1238 to 1243 cm^{-1} confirms successful crosslinking of copolymer on to the PSF substrate, and presence of a low intensity stretching frequency at 1718 cm^{-1} appeared in all the cases confirms the presence of carbonyl (-C=O) groups (of unreacted GA) which, indicates chemical modification and crosslinking of active layer of PVA-*co*-SSA by GA[35,36] rested onto the PSF membrane. The broad band at around 3400 cm^{-1} reveals the availability of -OH and – SO_3H groups of constituting repeat units of copolymer chain, and indicates the presence of a thin coating layer of GA modified PVA-*co*-SSA on the PSF substrate membrane. Fig. 4 shows the typical FT-Raman spectra for PSF substrate as well as PSF/PVA-*co*-SSA/GA based TFCM. As seen from Fig. 4(a), PVA showed various characteristics Raman shifts which includes -CH_2 bond-stretching (2930 cm^{-1}), and -CH_2 bending (1438 cm^{-1}), -C-O-C symmetric bond-stretching (1135 cm^{-1}), -C-C bond-stretching (854 cm^{-1}), and -OH bond wagging out-plane deformation (618 cm^{-1}) as reported in[33]; while PSSA (as shown in Fig. 4(b) exhibited Raman shifts for -CH stretching (at 3058 cm^{-1}), aromatic ring stretching (at 1597 cm^{-1}), -SO_2 asymmetric stretching (at 1195 cm^{-1}), and – SO_2 group vibrations (at 1127, 1035, and 633 cm^{-1}).[33]

The FT-Raman spectrum of PSF UF membrane (S0) is shown in Fig. 4(c) and (d) along with Raman spectra

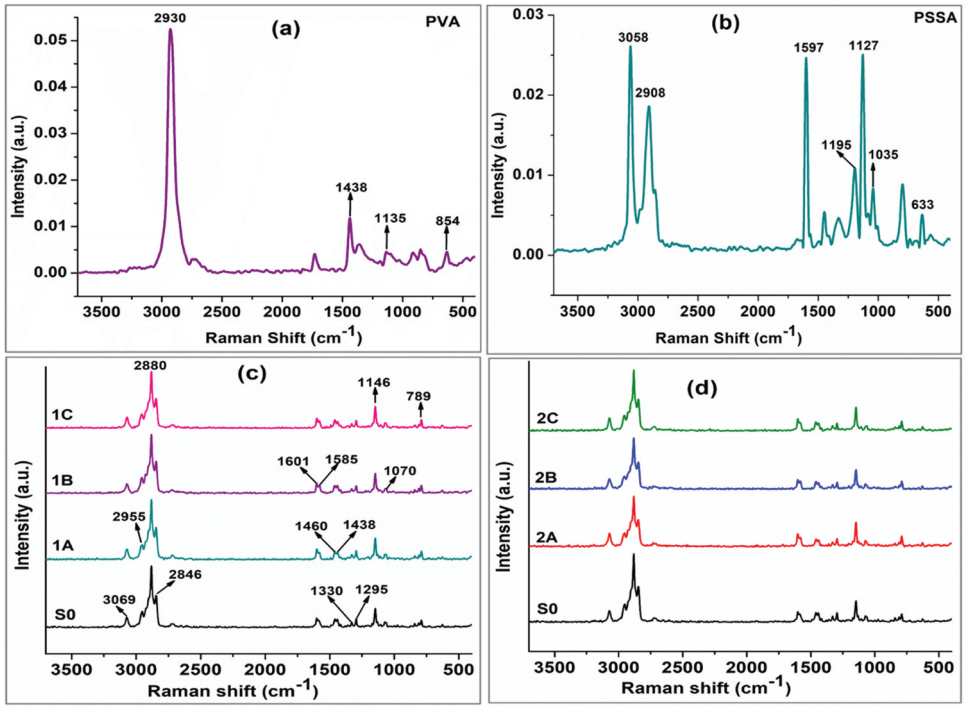


Figure 4. FT-Raman spectra of (a) PVA, and (b) PSSA, and (c and d) PSF/PVA-*co*-SSA/GA composite membranes i.e., 1A, 1B, and 1C, and 2A, 2B, and 2C, respectively.

of composite membranes. Typical characteristics Raman shift of PSF membrane appeared at 3069 cm^{-1} (–CH stretching),[37,38] 2955 cm^{-1} (-CH bond-stretching), 2880 and 2846 cm^{-1} (-C-CH_3 vibrations),[39] 1601 and 1585 cm^{-1} (assigned to the aromatic ring stretching),[38] 1460 and 1438 cm^{-1} (-CH_2 bending vibrations), 1295 and 1330 cm^{-1} (aliphatic chain stretching), 1146 cm^{-1} (-C-O-C bond-stretching) and at 790 cm^{-1} (asymmetric vibrations for –C-S-C).[37,38] However, a coating of crosslinked layer of PVA-*co*-SSA onto PSF substrate resulted in formation of composite membrane and observed Raman shift of such membranes are more intense and slightly shifted. Especially, aromatic ring vibrations at 1601 cm^{-1} seem sharper and clearer. It can be noticed that, -CH stretching, aromatic ring vibration, -C-O-C stretching, and – SO_2 vibrations at 3069, 1601, 1146, and 790 cm^{-1} respectively of PSF membrane gets overlapped and merged with homopolymers of PVA and PSSA stretching as shown in Fig. 4(a) and (b).

Surface water-wettability of PSF/PVA-co-SSA/GA TFCMs

Contact (or wetting) angle is significant in water treatment membranes, which indicates the spreadability/wettability of water on to the top surface of membrane and reveals its hydrophilic/hydrophobic features. Hydrophilic properties of membrane insight into fouling and water flux characteristics of the membrane. As depicted in Fig. 5(a), a bare PSF UF membrane showed water contact angle of 60.76° which, reveals its moderate hydrophilicity characteristics. Formation of thin selective layer using various concentrations of PVA-*co*-SSA and GA solution resulted in development of a hydrophilic thin-layer onto membrane surface that is well evidenced from the obtained values of contact angle. Composite membrane samples showed wetting angle in the range of 41° to 51°, as indicated in Fig. 5, this result suggests the formation of hydrophilic coating layer onto PSF membrane surface, however, there is no any specific trend observed in measured wetting angle with respect to change in concentration of PVA-*co*-SSA and GA solution used for membrane fabrication. Overall, hydrophilicity of the PSF membrane enhanced by immobilizing a thin selective layer of hydrophilic crosslinked polymer i.e., PVA-*co*-SSA, which is likely to enhance antifouling characteristics of membranes. Additionally, from the hydrophilic properties of membranes, further, it is clear that the trend in water flux and salts (NaCl and $MgSO_4$) rejection of membranes is expected to depend on the active layer thickness, morphology and crosslink characteristics, and solute and water affinity toward selective layer.

Morphology of PSF/PVA-co-SSA/GA TFCMs

Figure 6 shows the surface and cross-sectional topography of TFCM made from PVA-*co*-SSA and GA of varying the concentrations. As can be seen from the figure, the surface of bare PSF substrate exhibited planner nodular structure with nanoporous structure, while the top cross-sectional view appeared like microporous sponge type morphology that supported onto the fingers shaped porous supporting structure. The composites membrane surfaces overall displayed smooth appearance and seems to be covered with a thin selective layer. The cross-sectional views of all the TFCMs are

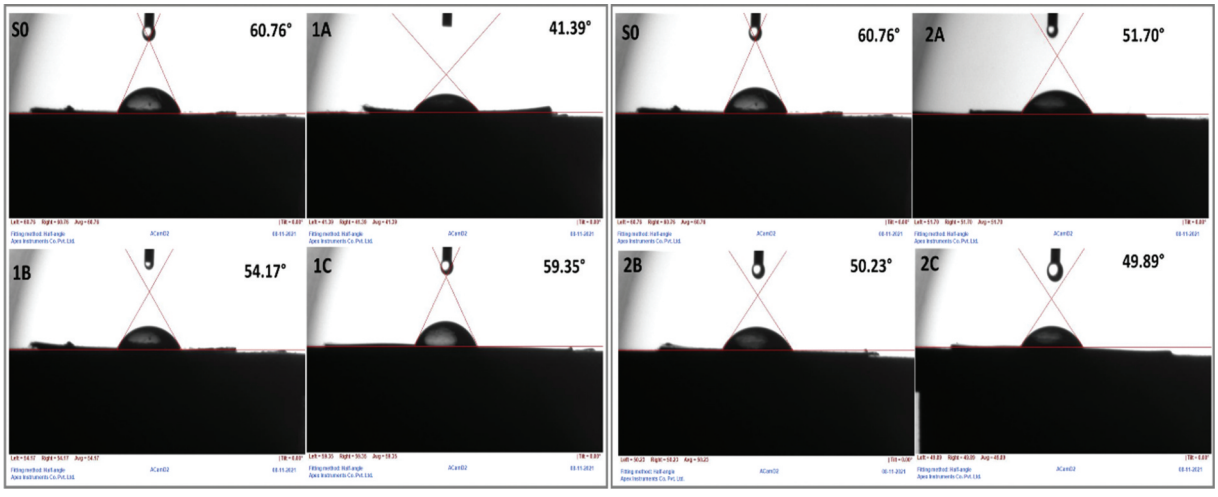


Figure 5. WCA measured on to top surface of bare PSF (S0) and PSF/PVA-co-SSA/GA composite membranes such as 1A, 1B, and 1C and 2A, 2B, and 2C.

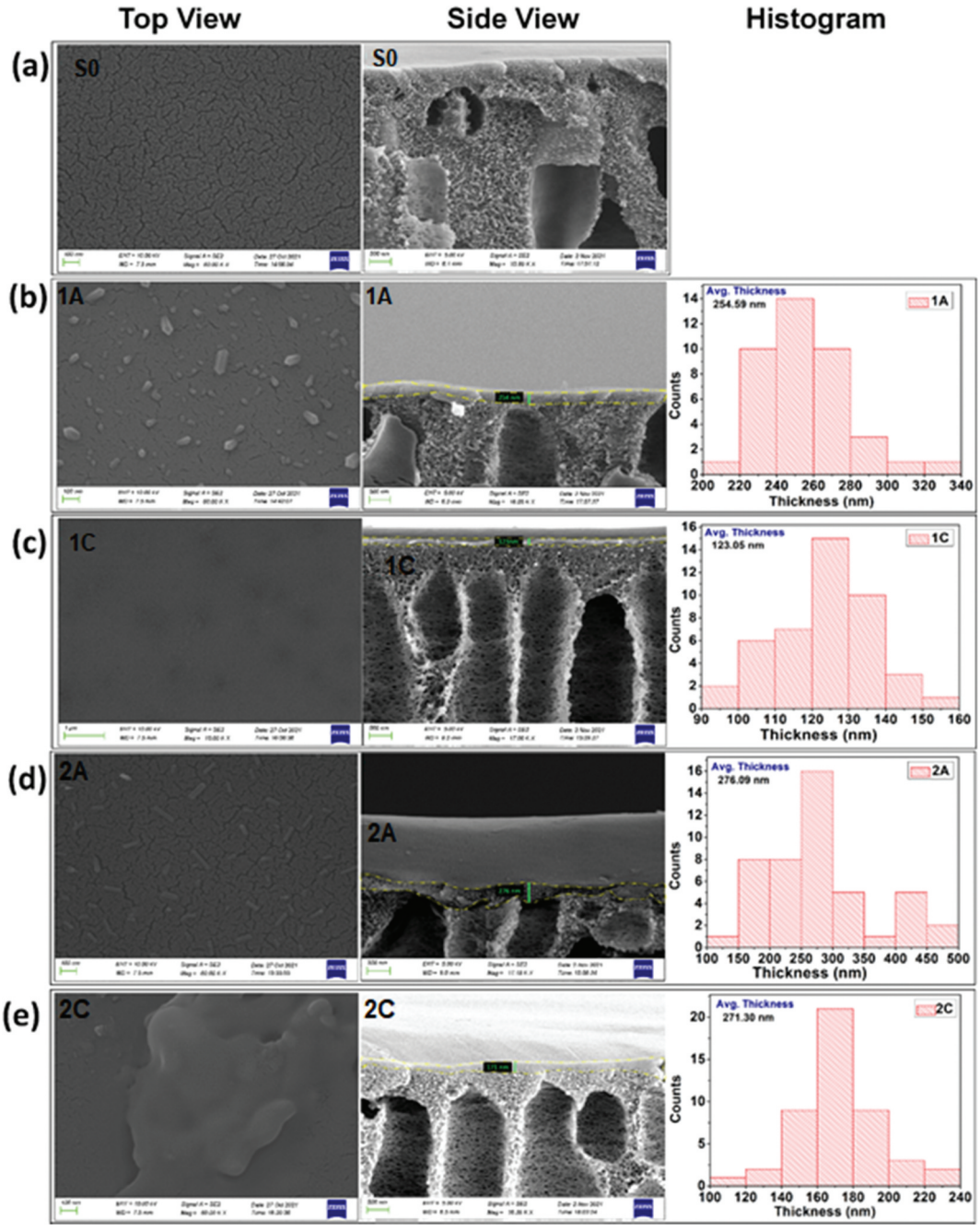


Figure 6. FE-SEM micrograph of the top and cross-sectional view of (a) bare PSF substrate, and (b-e) PSF/PVA-*co*-SSA/GA composite membranes i.e., 1A, 1C, 2A, and 2C, along with thickness histogram of the selective layer.

clearly distinguished from the bare PSF membrane. A clear and nanoscale top layer successfully produced by the aqueous solution of PVA-*co*-SSA/GA. The average thickness of coating layer calculated from the side view of the TFCMs are listed in Table 2. The active layer thickness of composite membrane prepared with higher concentration of PVA-*co*-SSA solution (1A) showed more thickness than membrane fabricated using low concentration of PVA-*co*-SSA (1C); while varying the concentration of GA solution for crosslinking keeping the PVA-*co*-SSA solution fixed for coating resulted in no significant change in active layer thickness of membranes.

Surface roughness of PSF/PVA-co-SSA/GA TFCMs

AFM analysis was carried out to find out roughness of the PSF/PVA-co-SSA/GA based TFCMs. Figures 7 and

Table 2. Surface roughness, average thickness, and zeta potential of PSF substrate and PSF/PVA-co-SSA/GA composite membranes.

Membranes	AFM, Roughness, rms (nm)	Average thickness (FE-SEM) (nm)	Zeta potential (mV)
S0	14.5±8.1	-	-
1A	20.9±14.4	254.59	−25.85
1C	20.7±13.1	123.05	−10.97
2A	24.9±9.9	276.09	−19.77
2C	26.3±11.4	271.30	−29.55

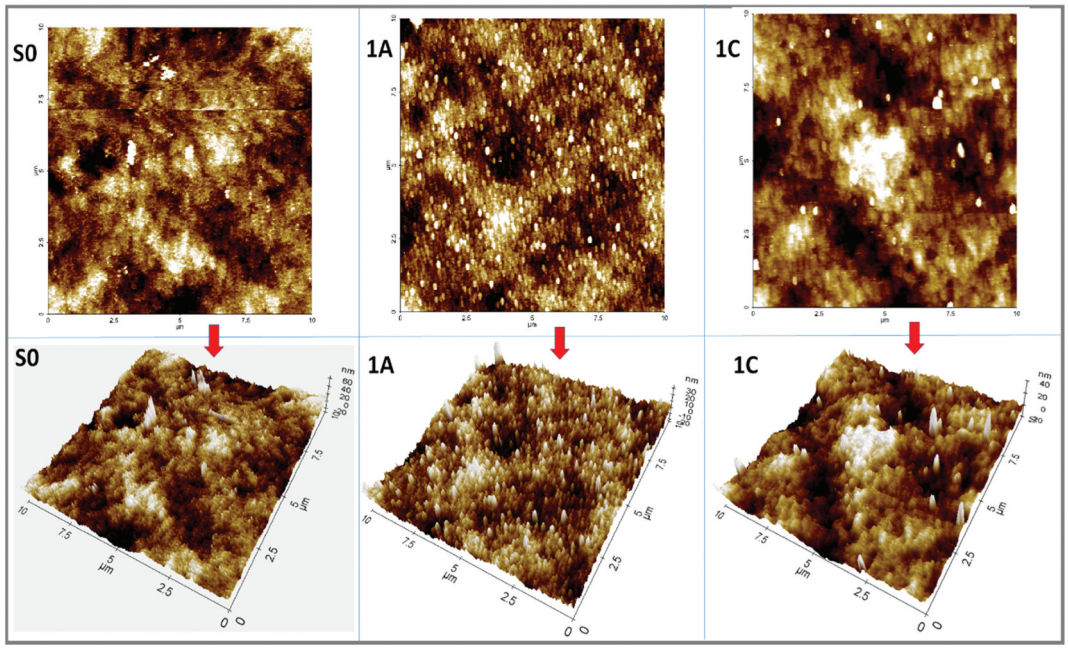


Figure 7. 2D and 3D AFM images of PSF (S0) and PSF/PVA-*co*-SSA/GA composite membranes (1A and 1C).

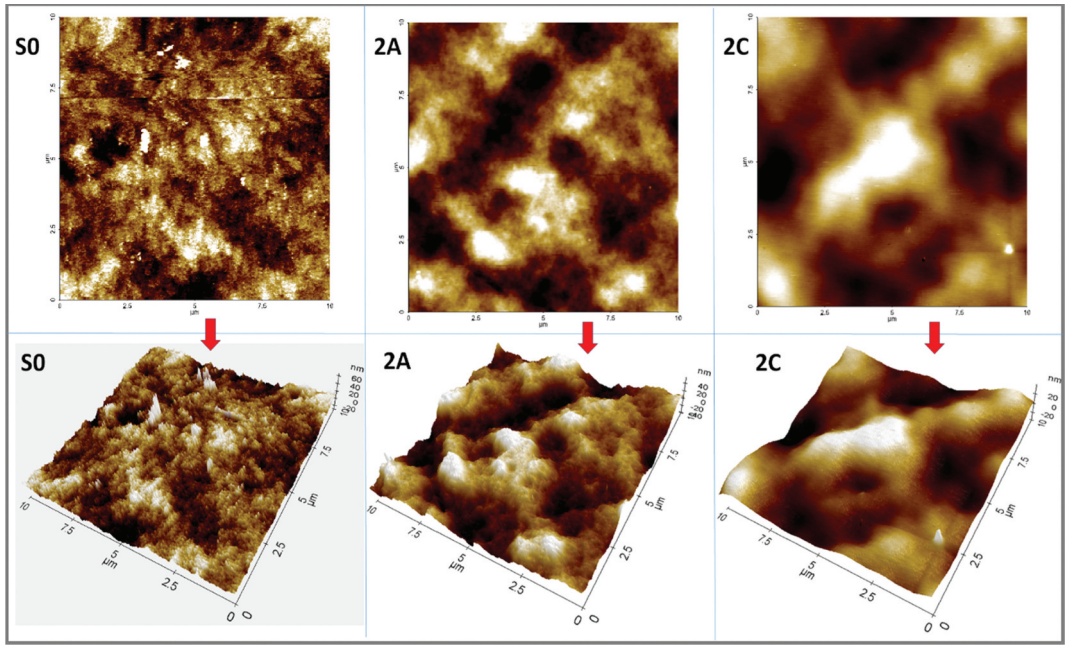


Figure 8. 2D and 3D AFM images of PSF (S0) and PSF/PVA-*co*-SSA/GA composite membranes (2A and 2C).

Fig. 8 show the 2D and 3D view of TFCM obtained by AFM analysis with 10 µm x 10 µm projection area. The PSF membrane (S0) shows surface roughness (rms 14.5 nm) (as shown in the Table 2). All composite membranes showed slightly higher roughness; however, these values of roughness indicate the formation smoother surface compared to conventional polyamide based TFC membranes.[40] From this results of surface roughness, this type of coating is expected to be helpful for chemical modification of conventional polyamide surface of TFCMs for reducing membrane surface roughness and fouling tendency.

Performance of PSF/PVA-co-SSA/GA TFCMs

Figure 9 and Fig. 10 represent water flux as well as bivalent salt ($MgSO_4$) rejection capacity of PSF/PVA-co-SSA/GA based TFCMs. As seen from the flux and rejection trend in Fig. 9, as the concentration of the PVA-*co*-SSA coating solution used for membrane preparation decreased from 2.5 to 1 wt.% (membrane sample 1A to 1C) the overall flux of membrane was increased while $MgSO_4$ rejection decreased. This is because of a thin selective-layer formation with decreasing coating solution concentration, which facilitated water transport due to lower mass transport resistance offered in thinner membrane compared to thick membrane, while decrement in $MgSO_4$ retention may be attributed to the formation of loose network structure that could be resulted in formation more porous/higher molecular weight cutoff membrane. Further, it is expected that NF membrane predominantly contains the partial salt-passage region, the absolute salt-passage region, and water-transport region,[41] that altogether coordinate the complex trade-off effect of salt rejection and water flux. Overall, membrane tested at 0.69 MPa operating pressure showed water flux in the range of 3.2 to 32.8 l m^{-2} h^{-1} and $MgSO_4$ rejection in the range of 74.8 to 60%; while similar membrane operated at higher pressure 1.70 MPa showed about 40% enhancement in water flux (in the range of 5.9 to 54.7 l m^{-2} h^{-1}) and $MgSO_4$ rejection (in the range of 66.2 to 79.2%). This enhanced water flux and $MgSO_4$ rejection obtained when membrane tested at high pressure is due

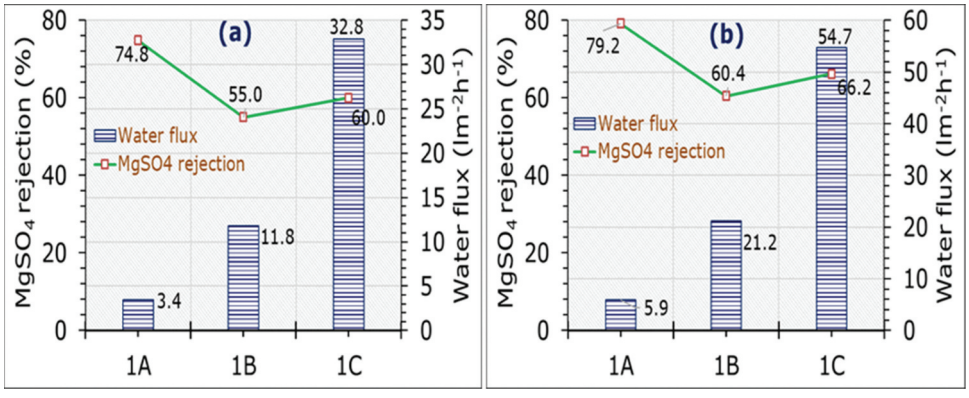


Figure 9. Water flux and $MgSO_4$ rejection of PSF/PVA-co-SSA/GA composite membrane (1A, 1B, and 1C) operated at (a) 0.69 MPa, and (b) 1.7 MPa (Feed solution 1000 ppm $MgSO_4$ solution).

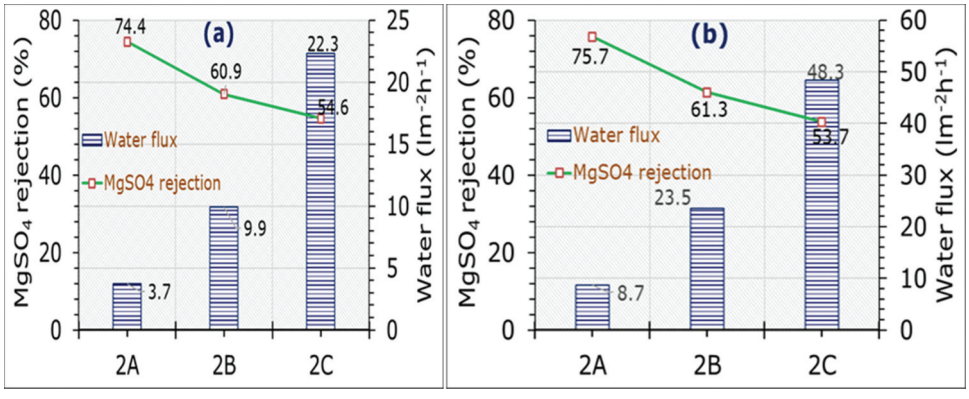


Figure 10. Water flux and $MgSO_4$ rejection of PSF/PVA-co-SSA/GA composite membrane (2A, 2B, and 2C) operated at (a) 0.69 MPa, and (b) 1.7 MPa (Feed solution 1000 ppm $MgSO_4$ solution).

to more preferential transport of water than bivalent salt ions.

Membranes obtained by coating PVA-*co*-SSA of 2 wt. % solution on PSF support and active layer crosslinked by varying GA solution of 6, 4, and 2 wt.% were designated as 2A, 2B, and 2C, respectively. Effect of GA solution concentration used for network formation, on flux and rejection properties of resultant composite membranes is indicated in Fig. 10. As expected, as the concentration of GA solution decreased from 6 to 2 wt. % (membrane 2A to 2C) improvement in water flux of membrane is observed, this is due to decrease in mass transport resistance through a thinner layer (as observed in SEM micrograph as shown in Fig. 6), while $MgSO_4$ rejection get decreased. Water flux obtained at 0.69 MPa for 2A, 2b, and 2C membrane was 3.7, 9.9, and 22.3 l m^{-2} h^{-1} respectively, while this value of water flux gets increased to 8.7, 23.5, and 48.3 l m^{-2} h^{-1}, respectively when operated at high pressure (1.7 MPa). Meanwhile, $MgSO_4$ rejection was not affected significantly and it was in the range of 74.4 to 54.6% and 75.7 to 53.7% when membrane tested at 0.69 and 1.7 MPa feed pressure, respectively.

Desalination performance of TFCMs was evaluated in the cross-flow test cell fed with 2000 ppm NaCl at feed pressure of 1.7 MPa is shown in Fig. 11. With increasing concentration of PVA-*co*-SSA solution (1C, 1B, and 1A in Fig. 11(a)) as well as GA solution concentration (2C, 2B, and 2A in Fig. 11(b)), the water flux of the membrane gets decreased while NaCl rejection enhanced. Overall, NaCl rejection (Fig. 11) is lesser than $MgSO_4$ rejection (Figs. 9 and 10) for all types of membranes. Since, the surface of composite membranes contains negatively charged -SO_3H groups, which are expected to provide more electrostatic repulsion to SO_4^{2-} ions compared to Cl^- anions. Studied membranes showed zetapotential value in the range of −29.55 to −19.77 mV, which was lower than controlled membrane, this indicates that membrane have negative surface charge. Moreover, hydrated radius of SO_4^{2-} (0.379 nm) is greater than Cl^- (0.332 nm) anion.[42] This implies that for the negatively charged membrane the more retention was attained for anions that have more hydrated radius and molecular weight. Beside that Cl^- have much lower hydration free energy (−340 kJ mol^{-1}) than SO_4^{2-} (−1040 kJ mol^{-1}) anions,[43] therefore, they can easily decrease the number of water-molecules in the hydration-shell and as a result, can pass readily through the membrane. Overall, membrane ions separation can be best explained by combined effect of Donnan exclusion, sieving effect and dielectric exclusion.[44] Meanwhile, water transport through the active crosslinked layer of PVA-co-SSA can be attributed to the formation of water channels constituted by the formation of nanopores structure (as seen from morphology of composite membranes' surface in Fig. 6). The deposition of more crosslinking agent i.e., GA or PVA-*co*-SSA onto membrane surface provided obstruction to water transport and increased the solute rejection due to formation of thicker or denser membrane (as seen from cross-sectional morphology of composite membranes in Fig. 6). There is a kind of trade-off relationship between membrane salt(s) rejection and water flux since the increment in salt rejection proportionally affected water flux of all composite membranes.

Typically, membrane sample 1C and 2C has been tested for 8 h in cross-flow cell to study the stability of membrane. After 8 h operation at constant 1.7 MPa pressure using 2000 ppm NaCl feed solution, the normalized water flux for 1C and 2C membrane samples slightly decreased by 1.9% and 2.6% while the normalized NaCl rejection has slightly increased by 1.2% and 1.1%, respectively. This indicates that this type of membranes is quite stable in aqueous

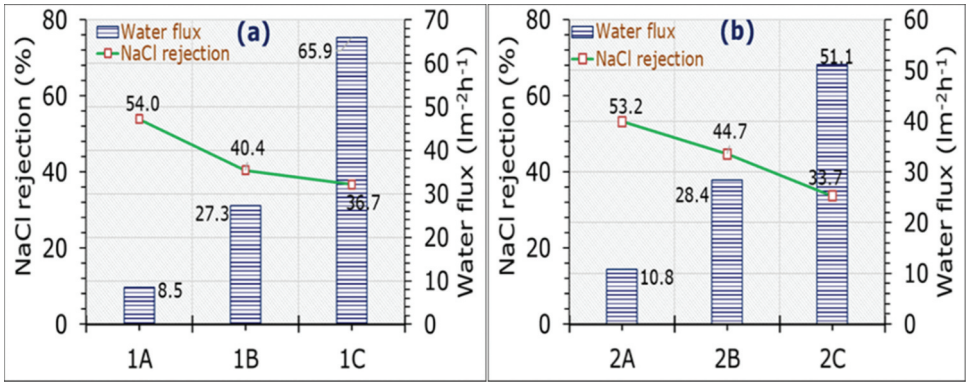


Figure 11. Water flux and NaCl rejection of PSF/PVA-co-SSA/GA composite membranes (a) 1A, 1B, and 1C, and (b) 2A, 2B, and 2C operated at 1.7 MPa (Feed: 2000 ppm NaCl solution).

medium and expected to be used for separation of ions, and moderate softening of water; further, it is expected that this type of membrane may be suitable for separation/removal of heavy metal ions from seawater as well as enrichment/separation of aqueous solution containing a mixture of inorganic and organic molecules.

Conclusions and future perspectives

Concept of preparation of composite membrane using PVA-*co*-SSA as an active/selective layer onto the PSF substrate has demonstrated following the conventional polyamide TFCM preparation approach. Composite membranes were successfully characterized to confirm presence of the active layer onto the PSF substrate by FTIR and FT-Raman spectroscopy. Besides that, water wetting angle, membrane morphology, and surface roughness characteristics of the composite membranes examined to correlate its structures and properties with the flux and rejection characteristics of TFCMs. Composite membranes had an active layer thickness in the range of 123 to 276 nm with smooth surface features. The maximum water flux was 54.21 m^{-2} h^{-1} at 1.7 MPa and 32.8 lm^{-2} h^{-1} at 0.69 MPa for the TFCM sample 1C, while the highest $MgSO_4$ obtained was 74.8 and 79.2% for TFCM sample 1A when operated at feed pressure of 0.69 and 1.7 MPa, respectively.

This study first time disclose a concept of preparation of TFCM using water soluble PVA-*co*-SSA and GA, and hence has a considerable future scope for further development. Performance of such type of membrane is expected to be improved by proper selection of support membrane, optimization of network formation, development of alternative coating technique, and incorporation of inorganic and organic additives. Further, determination of molecular weight cutoff would provide more insight into solute retention properties of membranes. This type of charged membrane anticipated to be suitable for separation of charged inorganic (ionic separation) and organic molecules from wastewater using membrane processes.

Acknowledgments

Authors (Gohil and Choudhury) acknowledge support from the Science and Engineering Research Board (SERB), New Delhi, India for the ECR Award (Project No. ECR/2017/000028). Authors acknowledge the "Analytical and Environmental Science Division and Centralized Instrument Facility, CSIR-CSMCRI" for instrument support.

Disclosure statement

No potential conflict of interest was reported by the author(s).

Funding

The work was supported by the Science and Engineering Research Board [ECR/2017/000028].

ORCID

Rikarani R Choudhury http://orcid.org/0000-0002-4319-578X
Jaydevsinh M. Gohil http://orcid.org/0000-0002-1262-6858
Hiren Raval http://orcid.org/0000-0002-8386-727X

Statement of novelty

This research work reports

- eco-friendly process for preparation of composite membranes
- novel TFC membranes based on poly(vinyl alcohol-*co*-styrenesulfonic acid) (PVA-*co*-SSA) functional copolymer
- the GA crosslinked-PVA-*co*-SSA/PSF composite membrane showed a trade-off relationship between salt rejection and water flux.
- TFC membrane had negative surface charge and gave higher bivalent salt rejection ($MgSO_4$) compared to monovalent salt (NaCl).

References

[1] Yang, Z.; Zhou, Y.; Feng, Z.; Rui, X.; Zhang, T.; Zhang, Z. A Review on Reverse Osmosis and Nanofiltration Membranes for Water Purification. *Polymers*. 2019, *11* (8), 1252. DOI: 10.3390/polym11081252.
[2] Seah, M. Q.; Lau, W. J.; Goh, P. S.; Tseng, H. H.; Wahab, R. A.; Ismail, A. F. Progress of Interfacial Polymerization Techniques for Polyamide Thin Film (Nano)composite Membrane Fabrication: A Comprehensive Review. *Polymers*. 2020, *12*(12), 2817. DOI: 10.3390/polym12122817.
[3] Farahbakhsha, J.; Vatanpourb, V.; Khoshnam, M.; Zargar, M. Recent Advancements in the Application of New Monomers and Membrane Modification Techniques for the Fabrication of Thin Film Composite Membranes: A Review. *React. Funct. Polym*. 2021, *166*, 105015. DOI: 10.1016/j.reactfunctpolym.2021.105015.
[4] Khoo, Y. S.; Lau, W. J.; Liang, Y. Y.; Yusof, N.; Ismail, A. F. Surface Modification of PA Layer of TFC Membranes: Does It Effective for Performance Improvement? *J. Ind. Eng. Chem*. 2021, *102*, 271–292. DOI: 10.1016/j.jiec.2021.07.006.
[5] Choudhury, R. R.; Gohil, J. M.; Mohanty, S.; Nayak, S. K. Antifouling, Fouling Release and

Antimicrobial Materials for Surface Modification of Reverse Osmosis and Nanofiltration Membranes. *J. Mater. Chem. A*. 2018, *6*(2), 313–333. DOI: 10.1039/C7TA08627J.

[6] Ji, C.; Zhai, Z.; Jiang, C.; Hu, P.; Zhao, S.; Xue, S.; Yang, Z.; He, T.; Niu, Q. J. Recent Advances in High-Performance TFC Membranes: A Review of the Functional Interlayers. *Desalination*. 2021, *500*, 114869. DOI: 10.1016/j.desal.2020.114869.

[7] Liang, D.; Yeung, Z. W.; Zhao, Q.; Chung, T. S. Thin-Film Nanocomposite Membranes Incorporated with UiO-66-NH_2 Nanoparticles for Brackish Water and Seawater Desalination. *J. Membr. Sci*. 2021, *604*, 118039. DOI: 10.1016/j.memsci.2020.118039.

[8] Choudhury, R. R.; Gohil, J. M.; Dutta, K. Poly(vinyl Alcohol)-Based Membranes for Fuel Cell and Water Treatment Applications: A Review on Recent Advancements. *Polym. Adv. Technol*. 2021, *32*(11), 4175–4203. DOI: 10.1002/pat.5431.

[9] Zhong, P. S.; Widjojo, N.; Chung, T. S.; Weber, M.; Maletzko, C. Positively Charged Nanofiltration (NF) Membranes via UV Grafting on Sulfonated Polyphenylenesulfone (sPPSU) for Effective Removal of Textile Dyes from Wastewater. *J. Membr. Sci*. 2012, *417-418*, 52–60. DOI: 10.1016/j.memsci.2012.06.013.

[10] Ding, J.; Wu, H.; Wu, P. Development of Nanofiltration Membranes Using Mussel-Inspired Sulfonated Dopamine for Interfacial Polymerization. *J. Membr. Sci*. 2020, *598*, 117658. DOI: 10.1016/j.memsci.2019.117658.

[11] Gumbi, N. N.; Li, J.; Mamba, B. B.; Nxumalo, E. N. Relating the Performance of Sulfonated Thin-Film Composite Nanofiltration Membranes to Structural Properties of Macrovoid-Free Polyethersulfone/Sulfonated Polysulfone/O-MWCNT Supports. *Desalination*. 2020, *474*, 114176. DOI: 10.1016/j.desal.2019.114176.

[12] Singh, A. K.; Thakur, A. K.; Shahi, V. K. Self-Assembled Nanofiltration Membrane Containing Antimicrobial Organosilica Prepared by Sol–Gel Process. *Desalination*. 2013, *309*, 275–283. DOI: 10.1016/j.desal.2012.10.011.

[13] Sangeetha, K.; Sudha, P. N.; Sukumaran, A. Novel Chitosan Based Thin Sheet Nanofiltration Membrane for Rejection of Heavy Metal Chromium. *Int. J. Biol. Macromol*. 2019, *132*, 939–953. DOI: 10.1016/j.ijbiomac.2019.03.244.

[14] Amiri, S.; Asghari, A.; Vatanpour, V.; Rajabi, M. Fabrication and Characterization of a Novel Polyvinyl Alcohol-Graphene Oxide-Sodium Alginate Nanocomposite Hydrogel Blended PES Nanofiltration Membrane for Improved Water Purification. *Sep. Purif. Techn*. 2020, *250*, 117216. DOI: 10.1016/j.seppur.2020.117216.

[15] Sapalidis, A. A. Porous Polyvinyl Alcohol Membranes: Preparation Methods and Applications. *Symmetry*. 2020, *12*(6), 960. DOI: 10.3390/sym12060960.

[16] El-Beharya, S. A.; El-Aassara, A. M.; Aboelfadla, M.; Abdel-Atey, N.; Kandil, A. T. Surface Modification of TFC Membranes Using PVA and Nanomaterials for Enhancing Fouling Resistance. *Desalinat. Water Treat*. 2020, *193*, 106–116. DOI: 10.5004/dwt.2020.25687.

[17] An, Q.; Li, F.; Ji, Y.; Chen, H. Influence of Polyvinyl Alcohol on the Surface Morphology, Separation and Anti-Fouling Performance of the Composite Polyamide Nanofiltration Membranes. *J. Membr. Sci*. 2011, *367*(1), 158–165. DOI: 10.1016/j.memsci.2010.10.060.

[18] An, Q.; Li, F.; Ji, Y.; Zhang, Z.; Chen, H. Study on Removal of Organic Matters in Water by PVA Modified PA-TFC Nanofiltration Membrane. *Desalinat. Water Treat*. 2011, *34*(1–3), 75–80. DOI: 10.5004/dwt.2011.2886.

[19] Shen, L. D.; Yu, X. F.; Cheng, C.; Yang, Y.; Wang, X. F.; Zhu, M. F. PVA-SA/PAN Thin-Film Nanofibrous Composite Membrane Prepared by Combining Electrospray Technique and Hot-Pressing Treatment. *Acta. PolymericaSinica*. 2017, *20*(5), 830–841. DOI: 10.11777/j.issn1000-3304.2017.16236.

[20] Bano, S.; Mahmood, A.; Kim, S. J.; Lee, K. H. Chlorine Resistant Binary complexedNaalg/PVA Composite Membrane for Nanofiltration. *Sep. Purif. Techn*. 2014, *137*, 21–27. DOI: 10.1016/j.seppur.2014.09.024.

[21] Zheng, Y.; Yao, G.; Cheng, Q.; Yu, S.; Liu, M.; Gao, C. Positively Charged Thin-Film Composite Hollow Fiber Nanofiltration Membrane for the Removal of Cationic Dyes Through Submerged Filtration. *Desalination*. 2013, *328*, 42–50. DOI: 10.1016/j.desal.2013.08.009.

[22] Wagh, P.; Parungao, G.; Viola, R. E.; Escobar, I. C. A New Technique to Fabricate High-Performance Biologically Inspired Membranes for Water Treatment. *Sep. Purif. Techn*. 2015, *156*, 754–765. DOI: 10.1016/j.seppur.2015.10.073.

[23] Soyekwo, F.; Liu, C.; Wen, H.; Hu, Y. Construction of an Electroneutral Zinc Incorporated Polymer Network Nanocomposite Membrane with Enhanced Selectivity for Salt/Dye Separation. *Chem. Eng. J*. 2020, *380*, 122560. DOI: 10.1016/j.cej.2019.122560.

[24] Gohil, J. M.; Ray, P. Polyvinyl Alcohol as the Barrier Layer in Thin Film Composite Nanofiltration Membranes: Preparation, Characterization, and Performance Evaluation. *J. Coll. Interf. Sci*. 2009, *338*(1), 121–127. DOI: 10.1016/j.jcis.2009.06.020.

[25] Dlamini, D. S.; Wang, J.; Mishra, A. K.; Mamba, B. B.; Hoek, E. M. V. Effect of Cross-Linking Agent Chemistry and Coating Conditions on Physical, Chemical, and Separation Properties of PVA-Psf Composite Membranes. *Sep. Sci. Technol*. 2014, *49*(1), 22–29. DOI: 10.1080/01496395.2013.813040.

[26] Miao, J.; Zhang, R.; Bai, R. Development and Characterization of Quaternized Poly (Vinyl Alcohol) Composite Nanofiltration Membranes. *J. Mater. Sci*. 2016, *51*(4), 1855–1863. DOI: 10.1007/s10853-015-9492-0.

[27] Kandeel, H. S.; Badawya, N. A.; Hamadaa, A. A.; El-Sayed, M.; Fathy, M.; Al-Gamal, A. A.; Moghny, T. A. Desalination Aspects of PSSA-G-PEG Copolymer and Its Graphene Composite Membranes. *Int. J. Chem. Sci*. 2018, *16*(3), 277. DOI: 10.21767/0972-768X.1000277.

[28] Cheong, S. I.; Kim, B.; Lee, H.; Rhim, J. W. Physical Adsorption of Water-Soluble Polymers on Hydrophobic Polymeric Membrane Surfaces via Salting-Out Effect. *Macromol. Res*. 2013, *21*(6), 629–635. DOI: 10.1007/s13233-013-1075-9.

[29] Hu, D.; Xu, Z. L.; Wei, Y. M.; Liu, Y. F. Poly(styrene Sulfonic Acid) Sodium Modified Nanofiltration Membranes with Improved Permeability for the Softening of Highly Concentrated Seawater. *Desalination*. 2014, *336*, 179–186. DOI: 10.1016/j.desal.2013.11.025.

[30] Polisetti, V.; Ray, P. Thin Film Composite Nanofiltration Membranes with Polystyrene Sodium Sulfonate–Polypiperazinetrimesamide Semi-Interpenetrating Polymer Network Active Layer. *J. Appl. Polym. Sci*. 2020, *137*(44), 49351. DOI: 10.1002/app.49351.

[31] Zhang, Y.; Zhao, C.; Yan, H.; Pan, G.; Guo, M.; Na, H.; Liu, Y. Highly Chlorine-Resistant Multilayer Reverse Osmosis Membranes Based on Sulfonated Poly (Arylene Ether Sulfone) and Poly (Vinyl Alcohol). *Desalination*. 2014, *336*, 58–63. DOI: 10.1016/j.desal.2013.12.034.

[32] Zhang, Y.; Wan, Y.; Pan, G.; Shi, H.; Yan, H.; Xu, J.; Guo, M.; Wang, Z.; Liu, Y. Surface Modification of Polyamide Reverse Osmosis Membrane with Sulfonated Polyvinyl Alcohol for Antifouling. *Appl. Surf. Sci*. 2017, *419*, 177–187. DOI: 10.1016/j.apsusc.2017.05.047.

[33] Choudhury, R. R.; Gohil, J. M.; Mohanty, S.; Nayak, S. K. Synthesis and Characterization of Novel Functional Poly (Vinyl Alcohol-Co-Styrene Sulfonic Acid) Copolymers. *Int. J. Polym. Anal. Charact*. 2019, *24*(4), 334–345. DOI: 10.1080/1023666X.2019.1596367.

[34] Singh, K.; Devi, S.; Bajaj, H. C.; Ingole, P.; Choudhari, J.; Bhrambhatt, H. Optical Resolution of Racemic Mixtures of Amino Acids Through Nanofiltration Membrane Process. *Sep. Sci. Technol*. 2014, *49*(17), 2630–2641. DOI: 10.1080/01496395.2014.911023.

[35] Gohil, J.; Karamanev, D. G. Novel Pore-Filled Polyelectrolyte Composite Membranes for Cathodic Microbial Fuel Cell Application. *J. Power Sources*. 2013, *243*, 603–610. DOI: 10.1016/j.jpowsour.2013.06.001.

[36] Rudra, R.; Kumar, V.; Kundu, P. P. Acid Catalysed Cross-Linking of Poly Vinyl Alcohol (PVA) by Glutaraldehyde: Effect of Crosslink Density on the Characteristics of PVA Membranes Used in Single Chambered Microbial Fuel Cells. *Rsc. Adv*. 2015, *5* (101), 83436–83447. DOI: 10.1039/C5RA16068E.

[37] Ionita, M.; Pandele, A. M.; Crica, L. E.; Obreja, A. C. Preparation and Characterization of Polysulfone/ammonia-Functionalized Graphene Oxide Composite Membrane Material. *High Perform. Polym*. 2016, *28*(2), 181–188. DOI: 10.1177/0954008315576233.

[38] Kim, H. J.; Fouda, A. E.; Jonasson, K. In situ Study on Kinetic Behavior During Asymmetric Membrane Formation via Phase Inversion Process Using Raman Spectroscopy. *J. Appl. Polym. Sci*. 2000, *75*(1), 135–141. DOI: 10.1002/(SICI)1097-4628(20000103)75:1<135:AID-APP15>3.0.CO;2-9.

[39] Lawson, E. E.; Edwards, H. G.; Johnson, A. F. FT Raman Spectroscopic Study of the Wavenumber Region 2800-2630 cm^{-1} of Selected Organic Compounds. *Spectrochim. Acta, Part A: Mol. Biomol. Spectrosc*. 1995, *51*(12), 2057–2066. DOI: 10.1016/0584-8539(95)01492-9.

[40] Gohil, J. M.; Suresh, A. K. A Statistical Study of the Effect of Preparation Conditions on the Structure and Performance of Thin Film Composite Reverse Osmosis Membranes. *Desalinat. Water Treat*. 2016, *57*(7), 2924–2941. DOI: 10.1080/19443994.2014.983181.

[41] Zhang, R.; Tian, J.; Gao, S.; Van der Bruggen, B. How to Coordinate the Trade-Off Between Water Permeability and Salt Rejection in Nanofiltration? *J. Mater. Chem. A*. 2020, *8*(18), 8831–8847. DOI: 10.1039/D0TA02510K.

[42] Nightingale, E. R. Phenomenological Theory of Ion Solvation. Effective Radii of Hydrated Ions. *J. Phys. Chem*. 1959, *63*(9), 1381–1387. DOI: 10.1021/j150579a011.

[43] Andersson, M. P.; Stipp, S. L. S. Predicting Hydration Energies for Multivalent Ions. *J. Comput. Chem*. 2014, *35*(28), 2070–2075. DOI: 10.1002/jcc.23733].

[44] Tomczak, W. The Application of the Nanofiltration Membrane NF270 for Separation of Fermentation Broths. *Membranes*. 2022, *12*(12), 1263. DOI: 10.3390/membranes12121263.